Forward signaling by EphB1/EphB2 interacting with ephrin-B ligands at the optic chiasm is required to form the ipsilateral projection

George Chenaux and **Mark Henkemeyer**[*]

Department of Developmental Biology and Kent Waldrep Foundation Center for Basic Research on Nerve Growth and Regeneration University of Texas Southwestern Medical Center 6000 Harry Hines Blvd. Dallas, TX 75390-9133, United States of America

Abstract

EphB receptor tyrosine kinases direct axonal pathfinding through interactions with ephrin-B proteins following axon-cell contact. Since EphB:ephrin-B binding leads to bidirectional signals, the contributions of signaling into the Eph-expressing cell (forward signaling) or the ephrin-expressing cell (reverse signaling) cannot be assigned using traditional protein-null alleles. To determine if EphB1 is functioning solely as a receptor during axon pathfinding, a new knock-in mutant mouse was created, $EphB1^{\text{T-lacZ}}$, that expresses an intracellular-truncated EphB1-β-gal fusion protein from the endogenous locus. As in the $EphB1^{-/-}$ protein-null animals, the $EphB1^{\text{T-lacZ/T-lacZ}}$ homozygotes fail to form the ipsilateral projecting subpopulation of retinal ganglion cell axons. This indicates that reverse signaling through the extracellular domain of EphB1 is not required for proper axon pathfinding of retinal axons at the optic chiasm. Further analysis of other *EphB* and *ephrin-B* mutant mice shows that EphB1 is the preferred receptor of ephrin-B2 and, to a lesser degree, ephrin-B1 in mediating axon guidance at the optic chiasm despite the coexpression of EphB2 in the same ipsilaterally projecting retinal axons.

Keywords

Axon guidance; binocular vision; EphB receptor; ephrin-B ligand; mouse

Introduction

Retinal ganglion cell (RGC) axons navigate defined pathways from each eye to reach their termination zones in select brain regions including the lateral geniculate nucleus (LGN). The optic chiasm is the midline choice point where RGC axons decide which hemisphere of the brain to target, as a subset target the ipsilateral over the contralateral hemisphere (Godement *et al.*, 1990; Sretavan, 1990; Hirai *et al.*, 2002). These ipsilateral projections are present in animals with binocular vision, where two eyes with an overlapping field of view allow stereoscopic vision (Blake & Wilson, 2010). In mice, the loss of EphB1 causes nearly all RGC axons to decussate resulting in a greatly diminished ipsilateral projection (Williams *et al.*, 2003). Recent data has suggested EphB1 forward signaling is necessary and sufficient to determine axon laterality at the optic chiasm midline (Williams *et al.*, 2003; Petros *et al.*, 2009; Rebsam *et al.*, 2009; Garcia-Frigola & Herrera, 2010). However, we show here that EphB1 is expressed not only in the RGCs but also within the chiasm region; therefore, a role

---

[*]Corresponding Author: Mark Henkemeyer, PhD, Fax 214-648-1960, Tel: 214-645-5916, mark.henkemeyer@utsouthwestern.edu.
Conflict of interest: The authors declare no conflicts of interest or financial interests.

for EphB1-stimulated reverse signaling in the directing of retinal axons at the chiasm cannot be excluded.

Eph receptor tyrosine kinases and their ephrin ligands are divided into two subclasses, A and B. B-subclass ephrins are transmembrane proteins that in general bind and activate EphB receptors (Murai & Pasquale, 2003; Himanen *et al.*, 2007). When ephrin-B-expressing cells contact EphB-expressing cells, the molecules cluster (Himanen *et al.*, 2001; Kullander & Klein, 2002) and both EphB and ephrin-B intracellular domains become tyrosine phosphorylated. This induces a signaling cascade via activation of the EphB catalytic domain and recruitment of Src homology 2 (SH2) domain proteins (Wybenga-Groot *et al.*, 2001). The phosphorylated ephrin-B intracellular domain also recruits SH2 domain proteins, so both molecules have the ability to act as receptors to transduce signals into their respective cells (Holland *et al.*, 1996; Cowan & Henkemeyer, 2002; Egea & Klein, 2007). EphB:ephrin-B bidirectional signaling complicates analysis of Eph or ephrin protein-null mutant mice, as phenotypes found in null mutants could be due to loss of forward signaling, reverse signaling, or the combined loss of both signals.

In order to clarify the ligand and receptor roles of EphB1, we generated a new mutant mouse that expresses an intracellular truncated EphB1-β-gal fusion protein that is selectively unable to transduce canonical EphB1 forward signals. This model is analogous to the previously generated *EphB2*^lacZ mutation, which has helped identify where EphB2 is functioning as a ligand or a receptor (Henkemeyer *et al.*, 1996; Birgbauer *et al.*, 2001; Grunwald *et al.*, 2001; Hindges *et al.*, 2002; Dravis *et al.*, 2007). We show that EphB1 mediated activation of reverse signaling is not necessary to direct ventrotemporal RGC axons ipsilaterally at the optic chiasm through the ligands ephrin-B2 and, to a lesser degree, ephrin-B1. Additionally, we show that EphB2 forward signaling is also involved in forming the ipsilateral projection although its role is subservient to that of EphB1.

Materials and Methods

Generation of EphB1^T-lacZ mice

129 mouse strain genomic DNA was obtained from Invitrogen Mouse BAC DNA Library Pools (Invitrogen cat# 96021RG) by screening bacterial artificial chromosome (BAC) superpools and pools via PCR to find a BAC clone 209575, which included exon 6 to 16 of *EphB1*. A pL452 based minitargeting vector plasmid with a loxP flanked neo cassette (Liu *et al.*, 2003) was constructed. A bacterial *lacZ* sequence was inserted in frame within exon 9 immediately following the codon corresponding to murine EphB1 amino acid #578 (EphB1: …YSDKL-MARDD…: β-gal). Using recombineering the minitargeting vector was then inserted into the BAC, and a targeting vector (TV) was retrieved into the vector pL254 (based on pL253 including a diphtheria toxin-alpha negative selection expression cassette 5' of the left homology arm in addition to a tk negative selection cassette 3' of the right homology arm). The TV was electroporated into R1 strain mouse embryonic stem cells (Nagy *et al.*, 1993), and 960 embryonic stem colonies were screened by southern blot analysis at the 5' and 3' ends using PCR synthesized probes. One clone (2C1) exhibiting homologous recombination was identified and injected into blastocysts. Resulting chimeric mice were mated and germline transmission of the initial *EphB1*^T-lacZ.Neo allele was verified by southern analysis, PCR (Fwd: tgaatcctctgcccaagggaatgt, Rev mutant: gaaacgccgagttaacgccatcaa (660 bp), Rev wild-type: tgcagaaggtaatcttccaccagg (450bp)), and sequencing. The loxP flanked neo cassette was removed by crossing *EphB1*^T-lacZ.Neo mice to a transgenic mouse that expresses Cre-recombinase in the germline, which generated the *EphB1*^T-lacZ allele (supporting Fig. S1).

Mice and breeding

Other mice used in this study have been previously described: *EphB1*[lacZ] and *EphB1*^{−} (Williams *et al.*, 2003), *EphB2*^{−} and *EphB2*[lacZ] (Henkemeyer *et al.*, 1996), *ephrin-B1*[loxP] (Davy *et al.*, 2004), *ephrin-B2*[T] and *ephrin-B2*[lacZ] (Dravis *et al.*, 2004), *ephrin-B2*[loxP] (Gerety & Anderson, 2002), hGFAP[cre] (Zhuo *et al.*, 2001), nestin[cre] (Tronche *et al.*, 1999), *ephrin-B2*[6YFΔV] (Thakar *et al.*, Submitted), and *ephrin-B3*[lacZ] and *ephrin-B3*[−] (Yokoyama et al., 2001). *Ephrin-B1*[−] null mutants were generated by crossing the *ephrin-B1*[loxP] conditional mice to a transgenic mouse that expresses Cre-recombinase in the germline. All mice were housed in the Animal Resource Center at the University of Texas Southwestern Medical Center at Dallas and the experiments on them followed protocols approved by the Institutional Animal Care and Use Committee.

Biotinylation assay

Primary cells were harvested from E13.5 fetuses by dissociating with trypsin and culturing *in vitro* for 24 hours. Cell surface proteins were then exposed and covalently linked to biotin by the addition of sulfo-NHS-SS-biotin (Pierce, Rockford, IL, USA), and total cell protein lysates were then prepared in lysis buffer (1% Triton, 100mM NaCl, 50mM NaF, 50mM Tris-HCl pH 7.5) containing Complete (Roche, Indianapolis, IN, USA) protease inhibitor cocktail. Streptavidin coated beads (Pierce) were used to pull down all biotinylated cell surface proteins, which were resolved on 6% Tris-glycine gels, transferred to PVDF (Millipore) membranes, and then immunoblotted with rabbit α-β-gal (1:1000 Millipore, Billerica, MA, USA), goat α-EphB2 (1:2000 R&D Systems, Minneapolis, MN, USA) (Dravis & Henkemeyer, 2011), and mouse α-β-actin (1:5000 Sigma) antibodies followed by secondary antibodies conjugated to horseradish peroxidase (1:500–2000 Jackson Immunoresearch, West Grove, PA, USA). α-β-gal specificity was confirmed by comparing protein lysates of WT to *EphB1*[T-lacZ] mutants.

X-gal staining

To stain embryos as whole mounts, pregnant females containing fetuses at the desired time-points where the day of plug day was considered embryonic day 0.5 (E0.5) were euthanized with CO_2 and specimens were removed, washed in wash buffer (2mM $MgCl_2$, 0.02% nonidet-P40, 0.1M PO_4 pH 7.3) fixed for 20 minutes at room temperature (RT) in fixative buffer (2% gluteraldehyde, 2mM $MgCl_2$, 5mM EGTA, 0.1M PO_4 buffer pH 7.3), and then placed in X-gal solution (wash buffer w/ 1mg/mL X-gal (Roche), 2.12 mg/mL $K4[Fe(CN)6] \cdot 3H_2O$, 1.64 mg/mL $K3[Fe(CN)6]$ (Sigma)) o/n at 37 °C. Specimens were washed, postfixed in 4% paraformaldehye (PFA) in PO_4 buffer o/n at RT, and were then dehydrated and clarified using methyl salicylate (Polysciences Inc., Warrington, PA, USA) prior to imaging.

To stain cryosections, unfixed brain tissue was quickly harvested and frozen under OCT medium or else cryopreserved in 30% sucrose in 0.1M PO_4 buffer pH 7.3 prior to freezing. Tissue was then sectioned on a cryostat (10 to 25 µm), immediately mounted on charged slides, and allowed to air dry. Sections were then washed in phosphate buffered saline with 0.1% Triton X-100 (PBS-TX100) and placed in X-gal solution o/n at 37 °C. Slides were washed, post-fixed in 4% PFA, counterstained with nuclear fast red, dehydrated with ethanol and then xylene, and imaged under an Olympus BX50 microscope.

Immunohistochemistry

E16.5 mouse brains were prepared and sectioned as mentioned above at 16 µm. Tissue was fixed in 1% PFA for five minutes, washed in PBS-TX100 two times for 5 minutes, blocked in 5% donkey serum (Gemini, Sacramento, CA, USA), exposed to goat α-ephrin-B1 (1:100

R&D Systems) and rat α-L1 (1:250 Millipore) (Conway *et al.*, 2011) for one hour at RT in 5% donkey serum, washed 3×, exposed to cy5 donkey a-Goat and cy3 donkey a-rat (1:250 Jackson), and washed 3×. Slides were mounted with aquapolymount (Polysciences Inc.) and visualized under confocal microscopy using a Zeiss 510 LSM at 20× magnification. To create the images shown, four 20× images from the same slide were combined using the software Panavue Image Assembler. Specificity for the α-ephrin-B1 antibody was confirmed by comparing the staining pattern of WT to *ephrin-B1*$^{-/-}$ littermates.

Anterograde labeling the LGN

For cholera-toxin subunit B (CTB) labeling, three unique strain combinations groups were used, 50% 129/ 50% CD1 (all brown pigmented mice), 90% CD1/ 10%129 strain (25% brown pigmented, 50% gray pigmented, and 25% albino mice), and 100% CD1 (all albino mice) (More information about coat color alleles available at http://jaxmice.jax.org/jaxnotes/index.html). Each group was analyzed independently. Adult mice 8–12 weeks of age were anaesthetized with ketamine/xylazine and injected with 2–4 µL of 0.5% CTB-AlexaFluor 555 (red) in PBS in the right eye and CTB-488 (green) in the left eye (Sigma C-22843 and C-22841, respectively). Tracer was allowed to undergo transport for two days and mice were cardiac perfused with 4% PFA. Brains were removed, post-fixed o/n, serially sectioned at 100 µm throughout entire LGN spanning ~1100 µm, and mounted in aquapolymount. The entire LGN for every mouse was visualized under confocal microscopy using a Zeiss 510 LSM at 10× magnification.

Retinal explant cultures

E15.5 fetuses that were wild-type (WT), *EphB1*$^{T-lacZ/T-lacZ}$, or *EphB1*$^{T-lacZ/T-lacZ}$: *EphB2*$^{-/-}$ had their retinas removed and explants isolated from either the most dorsal or ventral-temporal regions. Explants were grown for 16–24 hours on laminin and poly-O-ornithine coated glass coverslips in DMEM/F12 media supplemented with 1% BSA, insulin-transferrin-sodium selenite (Sigma cat# I1884), and 0.4% methylcellulose. Explants were then exposed to 250 µg/mL 5-bromo-6-chloro-3-indolyl-β-D-galactopyranoside (5–6 X-gal) (Sigma cat# B8931) to detect expression of EphB1-β-gal fusion protein for 1 hour at 37°C in media, washed 2× in PBS, fixed for 5 min in 4% PFA, washed 2× PBS-TX100, blocked in 5% donkey serum, immunostained with α-EphB2 (1:200), washed, exposed to cy3 donkey α-goat (1:250 Jackson) phalloidin conjugated to Alexa Fluor® 647 (1:50 Invitrogen #A22287) (Colvin *et al.*, 2010), and then imaged by confocal microscopy at 63× magnification. Specificity for the α-EphB2 antibody was confirmed by comparing staining in *EphB2*$^{-/-}$ null animals while specificity for the b-gal substrate was confirmed by comparing to WT tissue.

DiI labeling of optic chiasm

P0 mutant and wild-type littermates mice were anaesthetized on ice and decapitated. The eyelid was removed and heads placed in 4% PFA o/n. The lens and fixed aqueous humor was removed and a small crystal of DiI (Invitrogen #D3911) placed on the exposed optic disk. The head was place in PBS with 0.1% NaN$_3$ for 10 days until dye had diffused past optic chiasm. The ventral surface of the skull and meninges near optic chiasm were removed, and the ventral surface of the brain and optic chiasm were directly visualized on a Zeiss Stemi SV11 fluorescent microscope.

Statistical Methods

All images of LGN sections were quantified using ImageJ by measuring total pixel intensity of entire LGN's ipsilateral projection in one section and dividing the number by the corresponding contralateral measurements for matching tracer in contralateral LGN. All

experiments were performed simultaneously with WT littermates to reduce individual experimental biases. P-values were determined by student's t-test with 0.05 being the minimum criteria for statistical significance.

Results

Generation of *EphB1*[T-lacZ] mutant mice

To determine whether EphB1 functions as a receptor or a ligand to control the pathfinding of ipsilaterally-projecting RGC axons, a new knock-in mutant mouse was generated that replaces the region encoding the intracellular domain of EphB1 with an in-frame *lacZ* sequence encoding beta-galactosidase (β-gal). Previous studies from our laboratory have shown that similar *lacZ* mutant mice that express C-terminal truncated EphB2-β-gal, ephrin-B2-β-gal, and ephrin-B3-β-gal fusion proteins lose their ability to transduce cell autonomous signals that require the intracellular domain of the targeted protein (Henkemeyer *et al.*, 1996; Yokoyama *et al.*, 2001; Cowan *et al.*, 2004; Dravis *et al.*, 2004; Chumley *et al.*, 2007; Xu & Henkemeyer, 2009). However, unlike protein null mutants, these truncated EphB-β-gal and ephrinB-β-gal fusion proteins still retain their respective extracellular and transmembrane domains allowing them to be trafficked to the plasma membrane and act as ligands to stimulate reverse or forward signaling, respectively (see cartoon in Fig. 1A). Furthermore, since these truncated proteins are expressed from the endogenous genes, they are present at physiological spatial and temporal patterns. This eliminates artificial results that may be obtained by other methodologies (e.g. viral injection) where proteins are over-expressed, miss-expressed, or knocked down.

To create this new mutation, recombineering (Copeland *et al.*, 2001) was used to construct a targeting vector (TV) that inserted the *lacZ* open reading frame within the reading frame of *EphB1* exon 9 immediately following the codons encoding the transmembrane domain and before the juxtamembrane segment (Fig. 1B). The TV was electroporated into murine embryonic stem cells and homologous recombination generated an intermediate mutation, termed *EphB1*[T-lacZ.Neo], that was verified using southern blot analysis, PCR, and DNA sequencing (see Materials and Methods). Embryonic stem cells were then injected into blastocysts and resulting chimeric mice were crossed and screened for offspring that inherited the targeted allele. The loxP-flanked positive selection neomycin cassette was subsequently removed by crossing to a mouse that expresses Cre recombinase in the germline to generate *EphB1*[T-lacZ] mutant mice.

To validate β-gal expression from the *EphB1*[T-lacZ] mutation, embryos were collected at E10.5, E11.5, and E12.5 and stained as whole-mounts with X-gal. Expression of the EphB1-β-gal fusion protein was strong in the forebrain and hindbrain at E10.5, and at later stages intensified and broadened to include the midbrain and spinal cord (Supporting Fig. S1). The X-gal staining patterns observed here for the EphB1-β-gal fusion protein are consistent with the expected EphB1 expression pattern (Mori *et al.*, 1995).

EphB1-β-gal traffics to the cell surface

To verify that the C-terminal truncated EphB1-β-gal fusion protein is properly localized to the plasma membrane, cells from whole brains of E13.5 *EphB1*[+/T-lacZ] heterozygote mice and WT littermates were dissociated and cultured for 24 hours and then exposed to NHS-biotin to biotinylate all cell surface proteins. Total protein lysates were prepared and biotinylated proteins purified with strepavidin-coated beads. The biotinylated fraction and whole cell lysates were probed in immunoblots with antibodies against β-actin, EphB2, and β-gal. Functioning as a negative control, β-actin was only detected in the whole cell lysates indicating that the biotinylation specifically labeled only proteins exposed to the cell surface.

Serving as a positive control because it is trafficked to the cell surface, EphB2 was detected in both the whole-cell lysate and biotinylated fraction lanes. The truncated EphB1-β-gal fusion protein at the expected size of 180 kilodaltons was also present in both the whole-cell lysate and biotinylated fraction lanes from *EphB1*$^{+/\text{T-lacZ}}$ mice but not in the WT lanes (Fig. 1C). This demonstrates that the truncated EphB1-β-gal fusion protein traffics to the plasma membrane.

To investigate if the EphB1-β-gal fusion protein is transported throughout cellular processes, its expression pattern and subcellular localization was compared to the previously generated *EphB1*$^{\text{lacZ}}$ protein-null mutation, which expresses an unconjugated β-gal protein confined to the cell body. In X-gal stained sections of the adult hippocampus, both mutations reported expression of EphB1 within CA3 pyramidal neurons and neural progenitors in the subgranular zone of the dentate gyrus (Fig. 1D and E). Importantly, the β-gal staining observed in *EphB1*$^{\text{T-lacZ}}$ mice was visible in both the cell bodies and cellular processes including the axonal projections of the CA3 neurons that target the CA1 region and the cell body extensions of the subgranular zone progenitor cells that reach into the dentate molecular layer. This data shows the EphB1-β-gal fusion protein is transported into axons and other cellular processes.

Eph and ephrin expression patterns in the retina, optic nerve, and optic chiasm

In early stages of retinal axon pathfinding (up to E14.5 in mice), all RGC axons cross to the contralateral hemisphere, and then, around E15.5/E16.5 axons originating from the ventrotemporal portion of the retina are deflected from the main bundle at the optic chiasm to instead project to the ipsilateral side of the brain (Godement *et al.*, 1990; Sretavan, 1990). To better characterize when and where EphB1 and EphB2 may be functioning, the expression patterns of both receptors was examined at the retina, optic nerve, and optic chiasm by staining for the highly sensitive EphB1-β-gal and EphB2-β-gal fusion proteins. X-gal stains of horizontal cryosections of E16.5 mutant mouse embryos revealed highly localized expression in the temporal region of the ventral retina for EphB1-β-gal (Fig. 2A) while EphB2-β-gal was expressed throughout the ventral retina (Fig. 2B). EphB1-β-gal and EphB2-β-gal were also both visible throughout the length of the optic nerve (Fig. 2A' and B') and reached the optic chiasm. Here, EphB1 and EphB2 fusion proteins are present within the retinal axons of the chiasm, yet only EphB1 is also expressed in the area directly surrounding the chiasm (Fig. 2A" and B"). This data shows that both EphB1 and EphB2 are expressed in RGCs and are transported down their axons through the optic nerve to reach the optic chiasm. Therefore, they are both present when RGC axons are deciding which hemisphere to target.

The expression of ephrin-B1 around the optic chiasm was determined by comparing the staining pattern of an ephrin-B1 specific antibody in wild-type and *ephrin-B1*$^{-/\text{Y}}$ mouse embryo coronal sections at E16.5 (Fig. 2C and D, respectively). Wild-type embryos showed a pronounced ephrin-B1 staining pattern (blue) both within the optic chiasm and directly surrounding the lateral and ventral perimeter of the optic chiasm represented by L1 immunostaining (red). Additionally, the expression patterns of ephrin-B2-β-gal and ephrin-B3-β-gal fusion proteins were examined through X-gal staining as described above (Fig. 2E and F). This showed upregulated levels of ephrin-B2-β-gal fusion protein within and around the optic chiasm while the ephrin-B3-β-gal fusion protein remains more relegated to the ventral portion of the brain dorsal to the chiasm. This expression data indicate both ephrin-B1 and ephrin-B2, but not ephrin-B3, are expressed at the mid-line of the optic chiasm at E16.5.

Measuring minor changes in percentage of ipsilateral projections

In order to carefully examine the role of EphB1 and possibly of EphB2 in the formation of the ipsilateral RGC axon projection, a sensitive *in vivo* assay was used to measure the relative percentage of ipsilaterally projecting axons that reach the LGN. Using adult mice ~2 months of age, RGCs in the right eye were labeled with cholera-toxin subunit-B bound to AlexaFluor 555 (CTB-555, red), while RGCs in the left eye were simultaneously labeled with CTB-488 (green). After allowing the tracers to undergo anterograde transport for two days, the entire LGN of WT and mutant mice was visualized in serial coronal vibratome sections. Both the ipsilateral and contralateral projections are visible in one image where green in the left hemisphere LGN of each section represents the ipsilateral projections while red represents the contralateral projections, and vice versa for the corresponding right hemispheres.

To look for subtle differences in the percentage of ipsilateral to contralateral projections reaching the LGN, anterograde labeling was first carried out on WT mice with different pigments, for albino mice have a diminished percentage of RGC axons that project to the ipsilateral hemisphere (Drager, 1985; Jeffery, 2001). For our studies, we used combinations of two strains of mice, albino CD1 outbred mice and pigmented 129 inbred mice, which have four known alleles that effect coat color: white bellied agouti (A^w), pink eyed dilution (p), chinchilla (c^{ch}), and albino (c). When isolated, the coat colors for each of these mice are brown with dark eyes, light yellow with pink eyes, grey with dark eyes, and non-pigmented with pink eyes, respectively (Porter *et al.*, 1991; Bultman *et al.*, 1994; Brilliant, 2001; Steingrimsson *et al.*, 2006). Mice with brown coat color display a larger percentage of ipsilaterally projecting RGC axons reaching the LGN than mice with other pigmentation, which showed an overall decrease of 38% in ipsilaterally projecting RGC axons (Fig. 3A). This difference is statistically significant for the majority of the LGN, specifically for the more caudal portion of the LGN (Fig. 3B, p-value < 0.05, t-test). These data show that this method can be applied to quantify minor changes in the ability of RGC axons to target the ipsilateral LGN and suggests that the A^w allele partially regulates the ability of RGC axons to properly reach their correct hemisphere in the LGN. This is consistent with previous data that shows that non-pigmented rodents have developmental defects during retinal development that impairs neurogenesis and results in a diminished ipsilateral projection (Webster & Rowe, 1991; Rachel *et al.*, 2002). Important for this study, this data confirms the need to only compare animals in groups either possessing or lacking brown pigment.

$EphB1^{T\text{-}lacZ}$ mutants have a strongly reduced ipsilateral projection

When compared with WT littermates, $EphB1^{T\text{-}lacZ/T\text{-}lacZ}$ mutant mice displayed a strongly reduced ipsilateral projection that was equivalent to the $EphB1^{-/-}$ protein-nulls (Fig. 4A). Both mutant groups oeverall showed a statistically significant 90% decrease from WT throughout the entirety of the LGN (Fig. 4B, p-value < 0.05, t-test), and there was no statistically significant difference evident between these two groups (Fig. 4C). Thus, mice lacking the intracellular domain of EphB1 phenocopy $EphB1^{-/-}$ null mutant mice. This data strongly indicates that the intracellular domain of EphB1 is required to transduce forward signals necessary to deflect ventrotemporal RGC axons away from the optic chiasm such that they project ipsilaterally.

EphB1 and EphB2 are coexpressed on the same RGC axons

To determine whether EphB1 and EphB2 are coexpressed on the same RGC axons projecting from the ventrotemporal region of the retina, retinal explants from the dorsal and ventrotemporal regions of the retina were dissected at E15.5, cultured to promote axon outgrowth for 16–20 hours, and labeled for EphB1 and EphB2 expression. Due to the lack of a specific antibody for EphB1, this was not previously possible; however, with the truncated

EphB1-β-gal fusion, the inherent β-gal activity was used to specifically label EphB1 expressing axons by exposing cultured retinal explants to the substrate 5–6 X-gal (Mohler & Blau, 1996), which is converted in the presence of β-gal into an insoluble fluorescent byproduct. Cells were simultaneously labeled with an α–EphB2 antibody to identify EphB2 protein and Cy5-conjugated phalloidin to label all axonal projections.

While low expression of both EphB1 and EphB2 was detected in all axonal projections from explants taken from the dorsal region of the retina (Fig. 5A), higher levels of both EphB1 and EphB2 were present in axons from explants of the ventrotemporal region of the retina (Fig. 5B). While EphB2 expression was consistently elevated in all axons in the ventrotemporal explants, there were some axons with high relative levels of EphB1 and others with lower levels (Fig. 5B). As negative controls, explants from embryos that were $EphB2^{-/-}$ null did not show any axonal staining with the α–EphB2 antibody (Fig. 5C) and explants from animals WT for EphB1 did not show any β-gal related fluorescence on axonal projections or cell bodies (Fig. 5D). As the subset of EphB1 expressing RGC axons from the ventrotemporal explants also express EphB2, the potential exists for EphB2 to also function in guidance of axons at the optic chiasm.

The ipsilateral projection is more reduced in $EphB1^{T\text{-}lacZ}$: $EphB2^{lacZ}$ compound mutants

Because EphB2 is also expressed in ventral RGCs at the time their axons are being directed to the ipsilateral hemisphere and is highly conserved with EphB1 (Holash & Pasquale, 1995; Henkemeyer *et al.*, 1996; Birgbauer *et al.*, 2000), the potential role of this receptor was examined. Compared with $EphB1^{T\text{-}lacZ/T\text{-}lacZ}$ single mutants, $EphB1^{T\text{-}lacZ/T\text{-}lacZ}$:$EphB2^{lacZ/lacZ}$ compound mutants expressing two intracellular truncated EphB-β-gal fusion proteins showed a further 37% reduction in the percentage of ipsilaterally projecting RGC axons from WT where some sections of the LGN showed no visible ipsilateral projections remaining (Fig. 4A). This decrease in the ipsilateral projection of compound mutants was statistically significant when compared with $EphB1^{T\text{-}lacZ/T\text{-}lacZ}$ single mutants in 4 of the 9 sections through the LGN (Fig. 4C p-value < 0.05, t-test). This data suggests EphB2 may assist EphB1 in controlling RGC axon pathfinding decisions at the optic chiasm. In another group of mice analyzed separately because of coat color, no observable or significant difference between WT and $EphB2^{lacZ/lacZ}$ single mutant mice was found (supporting Fig. S2). Thus, unlike $EphB1^{T\text{-}lacZ/T\text{-}lacZ}$ single mutants, loss of the intracellular domain of EphB2 alone does not appear to affect the ipsilateral projection.

Reduced levels of EphB1 results in a diminished ipsilateral projection

To further explore this apparent interdependency of EphB1 and EphB2 for axon pathfinding at the optic chiasm, various combinations of mutant mice that were heterozygous for the $EphB1^{T\text{-}lacZ}$ mutation were analyzed. When compared to WT mice (Fig. 6A), $EphB1^{+/T\text{-}lacZ}$ heterozygote mutant mice displayed a 21% decrease in the ratio of ipsilaterally projecting RGCs visible throughout the LGN although the decrease was largely not statistically significant (Fig. 6B, p-value < 0.05, t-test). However, if the $EphB1^{+/T\text{-}lacZ}$ heterozygote mutants was compounded with the $EphB2^{lacZ/lacZ}$ forward signaling mutant mice, the relative percentage of ipsilateral to contralateral RGC axons was more strongly reduced by 64% in comparison to WT (Fig. 6A), and this difference was statistically significant through the majority of the LGN when compared to the $EphB1^{+/T\text{-}lacZ}$ heterozygote (Fig. 6B, p-value < 0.05, t-test). Importantly, this reduction in ipsilateral axons reaching the LGN was still not as drastic as the complete loss of the EphB1 intracellular domain alone (Fig. 6A), which showed a near complete ablation of the ipsilateral projection throughout the entirety of the LGN (Fig. 6B).

By examining mice that are heterozygous mutants for the EphB1-β-gal fusion protein, the amount of functional EphB1 forward signaling was reduced but not abolished. A trend for the reduction of ipsilaterally projecting axons to the LGN was then detectable, yet it was only when reduced levels of EphB1 were compounded in mutant mice also lacking the EphB2 intracellular domain that there was a statistically significant reduction in the percentage of ipsilateral axons projecting to the LGN. Still, mice with normal expression for EphB1 but lacking the intracellular domain of EphB2 displayed no difference in the ratio of ipsilateral to contralateral projections at the LGN compared to WT mice (supporting Fig. S2). Together, this genetic data indicates that EphB1 is the key regulator while EphB2 plays a supporting role in their function as receptors to deflect ventrotemporal RGC axons at the optic chiasm.

Conditional *ephrin-B1* and *ephrin-B2* mutant mice have reduced ipsilateral projection

In addition to examining EphB1 and EphB2, we also studied potential roles for ephrin-B1 and ephrin-B2 in formation of the ipsilateral projection using conditional knockouts. Since the population of cells that guide retinal axons at the midline are radial glial cells (Marcus *et al.*, 1995), two nervous system specific cre recombinase expressing transgenic mouse lines were used as drivers to delete floxed *ephrin-B1*^{loxP} and *ephrin-B2*^{loxP} alleles as outlined in Fig. 7 to generate single and double mutants. Similar results were obtained using either the human glial fibrillary acidic protein (hGFAP) or Nestin promoter transgenes that drive widespread cre expression in the developing mouse brain (Zhuo *et al.*, 2001; Tronche *et al.*, 1999; Messam *et al.*, 2000). In order to directly visualize ipsilateral and contralateral projections at the optic chiasm, a small crystal of DiI was placed on the optic disk of P0 mouse pups, and the dye was allowed to diffuse along the optic nerve. The optic chiasm was then exposed, and traced axons visualized. In hGFAP^{cre}: *ephrin-B1*$^{loxP/Y}$ or Nestin^{cre}: *ephrin-B1*$^{loxP/Y}$ mice (Fig. 7B and F), an ipsilateral projection is still evident comparable to control littermates (Fig. 7A and E). However, when either transgenic lines is combined with the *ephrin-B2*$^{T/loxP}$ mutations (Fig. 7C and G), the relative amount of ipsilaterally projecting retinal axons appears to be diminished. This phenotype is most evident in an hGFAP^{cre}: *ephrin-B1*$^{loxP/Y}$:*ephrin-B2*$^{T/loxP}$ double mutant mouse (Fig. 7D), where there are few ipsilateral projections remaining, a phenotype comparable to that seen in *EphB1*$^{T-lacZ/T-lacZ}$ single mutant mice (Fig. 7H). This suggests that conditional inactivation of ephrin-B1 and especially ephrin-B2 using these two cre drivers reduces the ipsilateral projection at the optic chiasm.

Ephrin-B1 and *ephrin-B2* mutant mice display a reduced ipsilateral projection

While the DiI labeling experiments demonstrate that loss of both ephrin-B1 and ephrin-B2 results in a decrease of ipsilateral projections from the optic chiasm, the respective roles of the ephrin-B molecules that are involved in directing the laterality of RGC axons was elaborated by using the sensitive LGN tracing method in adult mice described above. *Ephrin-B3*$^{-/-}$ null mice did not display a noticeable reduction in the ratio of ipsilaterally projecting RGCs compared to WT littermates (supporting Fig. S3). However, we found that *ephrin-B1*$^{-/Y}$ hemizygous male and *ephrin-B1*$^{-/-}$ null female mutant mice displayed a 31% decrease overall in the ratio of ipsilaterally projecting RGCs compared to WT that was statistically significant in 6 of the 9 sections (Fig. 8A,B, p-value < 0.05, t-test). While *ephrin-B2*$^{T/T}$ mice could not be analyzed, e*phrin-B2*$^{+/T}$ heterozygotes express less functional protein yet are still viable. These mice were found to exhibit a 19% decrease overall in the percentage of ipsilaterally projecting RGCs compared to WT (Fig. 8A), yet it was not statistically significant through most of the LGN (Fig. 8B, p-value < 0.05, t-test). These data suggest that ephrin-B1 and ephrin-B2 function in the proper pathfinding of ventrotemporal RGC axons while ephrin-B3 is not involved.

In addition to expression at the optic chiasm, ephrin-B2 is also expressed at high levels in the dorsal retina. To determine whether ephrin-B2 is functioning in guidance at the optic chiasm as a ligand to stimulate forward signaling or as a receptor to transduce reverse signals, mutant adult mice lacking the ability to transduce intracellular signals were also analyzed. The *ephrin-B2*$^{\text{lacZ/6Yf}\Delta\text{V}}$ reverse signaling mutant mice analyzed were viable adults and carried one copy of the lacZ allele that expresses an intracellular truncated ephrin-B2-β-gal fusion protein and one copy of the 6YFΔV mutant that has key point mutations within the intracellular domain of ephrin-B2 implicated in reverse signaling (the six tyrosines are replaced with phenylalanine and the C-terminal valine is deleted). This latter mutation produces a protein that can neither be tyrosine phosphorylated and bind SH2 domain containing proteins nor recruit PDZ domain containing proteins to its C-terminal tail (Thakar *et al.*, Submitted). Interestingly, the *ephrin-B2*$^{\text{lacZ/6Yf}\Delta\text{V}}$ mice exhibited, if anything, a slight 12% increase overall in the percentage of ipsilaterally projecting RGC axons (Fig. 8A.B). This indicates that reverse signaling is not necessary for guidance of ventrotemporal axons at the optic chiasm, and that perhaps either the truncated ephrin-B2-β-gal fusion protein or the ephrin-B2-6YFΔV mutant protein may have a slightly greater ability to stimulate forward signaling (see below). Nevertheless, ephrin-B2 does not require a functional intracellular domain to direct ventrotemporal RGC axons at the optic chiasm.

Discussion

The purpose of this study was to determine under *in vivo* conditions and expression levels if EphB1 functions as a ligand in its role in directing RGC axons to the ipsilateral hemisphere. A germline mutant mouse was created that removes the intracellular domain of EphB1 while leaving the extracellular and transmembrane domains unchanged. These *EphB1*$^{\text{T-lacZ/T-lacZ}}$ forward signaling mutant mice recapitulated the phenotype seen in *EphB1*$^{-/-}$ protein null mice, clearly illustrating that EphB1 dependent forward signaling, but not reverse signaling, is necessary to determine the laterality of RGC axons at the optic chiasm. Surprisingly, EphB2, which is also expressed on ventrotemporal RGC axons, is not required to deflect these axons unless the levels of EphB1 are also functionally reduced. Additionally, we found that genetic loss of ephrin-B1 and ephrin-B2 or reduction in ephrin-B2 decreases the percentage of RGC axons that project ipsilaterally, while the loss of ephrin-B2 mediated reverse signaling does not.

EphB1 forward signaling directs RGC axons to the ipsilateral hemisphere

Using a protein null mutant mouse, it was previously established that EphB1 directs ventrotemporal RGC axons at the optic chiasm to the ipsilateral hemisphere (Williams *et al.*, 2003), and it has been suggested that forward signaling regulates this (Petros *et al.*, 2009; Rebsam *et al.*, 2009; Garcia-Frigola & Herrera, 2010). Given the ability of EphB:ephrin-B interactions to activate both forward and reverse intracellular signals upon axon-cell contact and the high co-expression of EphB1 and ephrin-B2 at the chiasm, it was crucial to determine whether EphB1 is also functioning as a ligand in guidance at the optic chiasm. To directly address this, a mutant mouse was created that expresses an intracellular truncated fusion protein under the endogenous locus of EphB1. While the EphB1-β-gal fusion protein can still act as a ligand to stimulate ephrin-B reverse signaling, it cannot transduce a canonical forward signal that requires its intracellular domain. However, the truncated fusion protein does possess the potential to transduce a non-canonical forward signal, for EphB receptors interact in cis with the NR1 subunit of the NMDA receptor via the extracellular regions of both proteins without requiring the intracellular domain of EphB molecules (Dalva *et al.*, 2000; Grunwald *et al.*, 2001). Nevertheless, as the *EphB1*$^{\text{T-lacZ/T-lacZ}}$ mice recapitulate the phenotype seen in *EphB1*$^{-/-}$ null mice, our data demonstrate that canonical EphB1 reverse signaling is not required to deflect ventrotemporal

RGC axons at the optic chiasm. Interestingly, when this mutation was combined with an EphB2 forward signaling mutant mouse line, which display retinal axon pathfinding defects at the superior colliculus (Hindges *et al.*, 2002; Thakar *et al.*, Submitted), there was a sharper decrease in the percentage of ipsilateral to contralateral RGC axons reaching the LGN.

EphB1 and EphB2 are expressed on the same subset of ventrotemporal RGC axons

The increased defect seen in *EphB1/B2* double mutant mice suggests EphB1 and EphB2 have overlapping function, yet $EphB1^{\text{T-lacZ/T-lacZ}}$ mice display a phenotype while $EphB2^{\text{lacZ/lacZ}}$ mice do not. We sought to determine if EphB1 is distinctly expressed from EphB2 at the chiasm, as previous genetic studies have established some functional redundancy between EphB family receptors (Orioli *et al.*, 1996; Cowan *et al.*, 2000; Hindges *et al.*, 2002; Henkemeyer *et al.*, 2003; Chen *et al.*, 2004; Dravis *et al.*, 2004; Chumley *et al.*, 2007). By performing X-gal stains of developing tissue on the $EphB1^{\text{T-lacZ}}$ and $EphB2^{\text{lacZ}}$ mutant mouse reporters, axonal expression patterns of EphB1 and EphB2 can be seen within the optic nerve and at the optic chiasm when RGC axon laterality is being determined. However, to share redundant functions, both EphB1 and EphB2 must be expressed in the same cell, yet this was not previously determined due to a lack of a specific antibody against EphB1. Utilizing $EphB1^{\text{T-lacZ/T-lacZ}}$ mutants for retinal explant cultures, EphB1 and EphB2 are visibly co-expressed within the same ventrotemporal RGC fibers. Therefore, EphB2 has the potential to operate in a tandem with EphB1 at the chiasm.

EphB1 receptor is preferred over EphB2 at the optic chiasm

Even though EphB1 and EphB2 are co-expressed in these same ventrotemporal RGC axons, the inability of EphB2 to rescue function in $EphB1^{-/-}$ null and $EphB1^{\text{T-lacZ/T-lacZ}}$ mice implies that EphB2 is not required at the optic chiasm. However, mice that have reduced levels of functional EphB1 (i.e. $EphB1^{+/\text{T-lacZ}}$ heterozygotes) while expressing unaltered levels EphB2 display a close to normal ipsilateral population. When the $EphB1^{+/\text{T-lacZ}}$ heterozygote is compounded with $EphB2^{\text{lacZ/lacZ}}$, there is a statistically significant decrease in the percentage of ipsilaterally projecting RGCs. This shows that EphB2 does function in pathfinding at the chiasm, but only if the dosage of EphB1 is reduced. Moreover, $EphB1^{\text{T-lacZ/T-lacZ}}:EphB2^{\text{lacZ/lacZ}}$ compound mutants display an even stronger reduction in the percentage of ipsilaterally projecting axons than $EphB1^{\text{T-lacZ/T-lacZ}}$ single mutants. Alternatively, there exists the potential that truncated EphB2 is acting in a dominant negative manner in heterozygous $EphB1^{+/\text{T-lacZ}}$ mice, but this is unlikely, as truncated $EphB2^{\text{lacZ/lacZ}}$ single mutant mice have no discernible decrease in the percentage of ipsilaterally projecting RGC axons from WT mice. If the truncated form of EphB2 was functioning in a dominant negative fashion, a mild phenotype should be evident in these mice due to the impairment of EphB1 function. This genetic evidence suggests that EphB2 does possess a partial ability to guide axons at the chiasm, yet the role for EphB2 is subservient to EphB1.

Since the intracellular truncated *EphB1* and *EphB2* mutants both reduce ipsilateral ventrotemporal RGC projections, it is doubtful that the unique factor of EphB1 stems from the intracellular domain. Previous studies have shown that EphB-mediated axon retraction is heavily dependent upon the downstream regulation of Rho GTPases (Etienne-Manneville & Hall, 2002; Noren & Pasquale, 2004). Furthermore, blocking Rho-kinase signaling, which can be activated by EphB2 (Shi *et al.*, 2009), stops the retraction response of ventrotemporal RGC axons stimulated with ephrin-B2 (Petros *et al.*, 2010). Moreover, a likely direct downstream target of EphB1 at the chiasm is the Rho family GEF Vav2, which directly binds EphB2 (Cowan *et al.*, 2005). These data further indicate that the intracellular domain of EphB1 and EphB2 are both able to induce axon repulsion at the optic chiasm though Rho-

GTPase dependent signaling. In addition, it has been reported that a percentage of non-ventrotemporal RGCs ectopically transfected with WT EphB1 cDNA are redirected ipsilaterally (Petros *et al.*, 2009; Rebsam *et al.*, 2009; Garcia-Frigola & Herrera, 2010). When a chimeric protein composed of the extracellular domain of EphB2 and intracellular domain of EphB1 is expressed, the RGC axons are redirected at a reduced level similar to full length EphB2 (Petros *et al.*, 2009). This and our data suggest that the specifying factor in EphB1's ability to direct RGC axons at the optic chiasm may lie within the extracellular domain.

Ephrin-B1 and ephrin-B2 function as ligands at the chiasm

Initial studies in Xenopus were the first to reveal B-subclass ephrins play a critical role in directing RGC axon laterality (Nakagawa *et al.*, 2000). Later studies used *in situ* expression data and *in vitro* growth cone collapse assays to suggest that ephrin-B2 is functioning as the sole repulsive ligand at the optic chiasm to interact with ventrotemporal RGC axons (Williams *et al.*, 2003; Petros *et al.*, 2010). Our study reveals that both ephrin-B1 and ephrin-B2 function as ligands at the optic chiasm while ephrin-B3 appears uninvolved. This is suppported by the expression of ephrin-B1 and ephrin-B2 around the optic nerve and at the midline of the optic chiasm while ephrin-B3 expression remains relatively low within the chiasm. However, unlike the apparent dependency of EphB2 on EphB1, ephrin-B1 and ephrin-B2 both seem to be capable of stimulating a forward signal response independently. Thus, it is unlikely that the specification of EphB1 activation over EphB2 is dependent on a particular EphB:ephrin-B interaction. Furthermore, by examining conditional mutants, it was determined that the population of cells that direct retinal axons express both GFAP and Nestin before and/or while ephrin-B1 and ephrin-B2 are steering retinal axons to the ipsilateral hemisphere.

In further evidence of the importance of forward signaling, the statistically significant increase of ipsilaterally projecting RGC axons in the ephrin-B2 reverse signaling mutant mice may be due to a gain of function from the ephrin-B2 truncated β-gal mutant mice. β-gal naturally forms a tetramer (Appel *et al.*, 1965; Juers *et al.*, 2000), so the ephrin-B2 extracellular domain would be in a state that mimicked activated ephrin-B2 before binding EphB1. This pre-clustered ephrin-B2 extracellular domain possesses the potential to act as an improved ligand since clustering is a key factor in transducing a forward signal (Himanen *et al.*, 2007). Thus, RGC axons that would normally take a contralateral pathway may be redirected to the ipsilateral hemisphere from enhanced forward signaling.

Supplementary Material

Refer to Web version on PubMed Central for supplementary material.

Acknowledgments

Abbreviations

BAC	bacterial artificial chromosome
β-gal	beta-galactosidase
CTB	cholera-toxin subunit B

E	embryonic day
hGFAP	human glial fibrillary acidic protein
LGN	lateral geniculate nucleus
n	nasal
o/n	overnight
ON	optic nerve
OX	optic chiasm
PDZ	postsynaptic density, discs large, zona occludens
RGC	retinal ganglion cell
RT	room temperature
SH2	Src homology 2
t	temporal
TV	targeting vector
WT	wild-type

References

Appel SH, Alpers DH, Tomkins GM. Multiple Molecular Forms of Beta-Galactosidase. J Mol Biol. 1965; 11:12–22. [PubMed: 14255754]

Birgbauer E, Cowan CA, Sretavan DW, Henkemeyer M. Kinase independent function of EphB receptors in retinal axon pathfinding to the optic disc from dorsal but not ventral retina. Development. 2000; 127:1231–1241. [PubMed: 10683176]

Birgbauer E, Oster SF, Severin CG, Sretavan DW. Retinal axon growth cones respond to EphB extracellular domains as inhibitory axon guidance cues. Development. 2001; 128:3041–3048. [PubMed: 11532925]

Blake R, Wilson H. Binocular vision. Vision Res. 2010; 50:1–17. [PubMed: 19800910]

Brilliant MH. The mouse p (pink-eyed dilution) and human P genes, oculocutaneous albinism type 2 (OCA2), and melanosomal pH. Pigment Cell Res. 2001; 14:86–93. [PubMed: 11310796]

Bultman SJ, Klebig ML, Michaud EJ, Sweet HO, Davisson MT, Woychik RP. Molecular analysis of reverse mutations from nonagouti (a) to black-and-tan (a(t)) and white-bellied agouti (Aw) reveals alternative forms of agouti transcripts. Genes Dev. 1994; 8:481–490. [PubMed: 8125260]

Chen ZY, Sun C, Reuhl K, Bergemann A, Henkemeyer M, Zhou R. Abnormal hippocampal axon bundling in EphB receptor mutant mice. J Neurosci. 2004; 24:2366–2374. [PubMed: 15014111]

Chumley MJ, Catchpole T, Silvany RE, Kernie SG, Henkemeyer M. EphB receptors regulate stem/ progenitor cell proliferation, migration, and polarity during hippocampal neurogenesis. J Neurosci. 2007; 27:13481–13490. [PubMed: 18057206]

Colvin RA, Means TK, Diefenbach TJ, Moita LF, Friday RP, Sever S, Campanella GS, Abrazinski T, Manice LA, Moita C, Andrews NW, Wu D, Hacohen N, Luster AD. Synaptotagmin-mediated vesicle fusion regulates cell migration. Nat Immunol. 2010; 11:495–502. [PubMed: 20473299]

Conway CD, Howe KM, Nettleton NK, Price DJ, Mason JO, Pratt T. Heparan sulfate sugar modifications mediate the functions of slits and other factors needed for mouse forebrain commissure development. J Neurosci. 2011; 31:1955–1970. [PubMed: 21307234]

Copeland NG, Jenkins NA, Court DL. Recombineering: a powerful new tool for mouse functional genomics. Nat Rev Genet. 2001; 2:769–779. [PubMed: 11584293]

Cowan CA, Henkemeyer M. Ephrins in reverse, park and drive. Trends Cell Biol. 2002; 12:339–346. [PubMed: 12185851]

Cowan CA, Yokoyama N, Bianchi LM, Henkemeyer M, Fritzsch B. EphB2 guides axons at the midline and is necessary for normal vestibular function. Neuron. 2000; 26:417–430. [PubMed: 10839360]

Cowan CA, Yokoyama N, Saxena A, Chumley MJ, Silvany RE, Baker LA, Srivastava D, Henkemeyer M. Ephrin-B2 reverse signaling is required for axon pathfinding and cardiac valve formation but not early vascular development. Dev Biol. 2004; 271:263–271. [PubMed: 15223333]

Cowan CW, Shao YR, Sahin M, Shamah SM, Lin MZ, Greer PL, Gao S, Griffith EC, Brugge JS, Greenberg ME. Vav family GEFs link activated Ephs to endocytosis and axon guidance. Neuron. 2005; 46:205–217. [PubMed: 15848800]

Dalva MB, Takasu MA, Lin MZ, Shamah SM, Hu L, Gale NW, Greenberg ME. EphB receptors interact with NMDA receptors and regulate excitatory synapse formation. Cell. 2000; 103:945–956. [PubMed: 11136979]

Davy A, Aubin J, Soriano P. Ephrin-B1 forward and reverse signaling are required during mouse development. Genes Dev. 2004; 18:572–583. [PubMed: 15037550]

Drager UC. Birth dates of retinal ganglion cells giving rise to the crossed and uncrossed optic projections in the mouse. Proc R Soc Lond B Biol Sci. 1985; 224:57–77. [PubMed: 2581263]

Dravis C, Henkemeyer M. Ephrin-B reverse signaling controls septation events at the embryonic midline through separate tyrosine phosphorylation-independent signaling avenues. Dev Biol. 2011; 355:138–151. [PubMed: 21539827]

Dravis C, Wu T, Chumley MJ, Yokoyama N, Wei S, Wu DK, Marcus DC, Henkemeyer M. EphB2 and ephrin-B2 regulate the ionic homeostasis of vestibular endolymph. Hear Res. 2007; 223:93–104. [PubMed: 17158005]

Dravis C, Yokoyama N, Chumley MJ, Cowan CA, Silvany RE, Shay J, Baker LA, Henkemeyer M. Bidirectional signaling mediated by ephrin-B2 and EphB2 controls urorectal development. Dev Biol. 2004; 271:272–290. [PubMed: 15223334]

Egea J, Klein R. Bidirectional Eph-ephrin signaling during axon guidance. Trends Cell Biol. 2007; 17:230–238. [PubMed: 17420126]

Etienne-Manneville S, Hall A. Rho GTPases in cell biology. Nature. 2002; 420:629–635. [PubMed: 12478284]

Garcia-Frigola C, Herrera E. Zic2 regulates the expression of Sert to modulate eye-specific refinement at the visual targets. Embo J. 2010; 29:3170–3183. [PubMed: 20676059]

Gerety SS, Anderson DJ. Cardiovascular ephrinB2 function is essential for embryonic angiogenesis. Development. 2002; 129:1397–1410. [PubMed: 11880349]

Godement P, Salaun J, Mason CA. Retinal axon pathfinding in the optic chiasm: divergence of crossed and uncrossed fibers. Neuron. 1990; 5:173–186. [PubMed: 2383400]

Grunwald IC, Korte M, Wolfer D, Wilkinson GA, Unsicker K, Lipp HP, Bonhoeffer T, Klein R. Kinase-independent requirement of EphB2 receptors in hippocampal synaptic plasticity. Neuron. 2001; 32:1027–1040. [PubMed: 11754835]

Henkemeyer M, Itkis OS, Ngo M, Hickmott PW, Ethell IM. Multiple EphB receptor tyrosine kinases shape dendritic spines in the hippocampus. J Cell Biol. 2003; 163:1313–1326. [PubMed: 14691139]

Henkemeyer M, Orioli D, Henderson JT, Saxton TM, Roder J, Pawson T, Klein R. Nuk controls pathfinding of commissural axons in the mammalian central nervous system. Cell. 1996; 86:35–46. [PubMed: 8689685]

Himanen JP, Rajashankar KR, Lackmann M, Cowan CA, Henkemeyer M, Nikolov DB. Crystal structure of an Eph receptor-ephrin complex. Nature. 2001; 414:933–938. [PubMed: 11780069]

Himanen JP, Saha N, Nikolov DB. Cell-cell signaling via Eph receptors and ephrins. Curr Opin Cell Biol. 2007; 19:534–542. [PubMed: 17928214]

Hindges R, McLaughlin T, Genoud N, Henkemeyer M, O'Leary DD. EphB forward signaling controls directional branch extension and arborization required for dorsal-ventral retinotopic mapping. Neuron. 2002; 35:475–487. [PubMed: 12165470]

Hirai T, Ito Y, Arai M, Ota Y, Kojima T, Sato M, Miyake Y. Loss of stereopsis with optic chiasmal lesions and stereoscopic tests as a differential test. Ophthalmology. 2002; 109:1692–1702. [PubMed: 12208719]

Holash JA, Pasquale EB. Polarized expression of the receptor protein tyrosine kinase Cek5 in the developing avian visual system. Dev Biol. 1995; 172:683–693. [PubMed: 8612982]

Holland SJ, Gale NW, Mbamalu G, Yancopoulos GD, Henkemeyer M, Pawson T. Bidirectional signalling through the EPH-family receptor Nuk and its transmembrane ligands. Nature. 1996; 383:722–725. [PubMed: 8878483]

Jeffery G. Architecture of the optic chiasm and the mechanisms that sculpt its development. Physiol Rev. 2001; 81:1393–1414. [PubMed: 11581492]

Juers DH, Jacobson RH, Wigley D, Zhang XJ, Huber RE, Tronrud DE, Matthews BW. High resolution refinement of beta-galactosidase in a new crystal form reveals multiple metal-binding sites and provides a structural basis for alpha-complementation. Protein Sci. 2000; 9:1685–1699. [PubMed: 11045615]

Kullander K, Klein R. Mechanisms and functions of Eph and ephrin signalling. Nat Rev Mol Cell Biol. 2002; 3:475–486. [PubMed: 12094214]

Liu P, Jenkins NA, Copeland NG. A highly efficient recombineering-based method for generating conditional knockout mutations. Genome Res. 2003; 13:476–484. [PubMed: 12618378]

Marcus RC, Blazeski R, Godement P, Mason CA. Retinal axon divergence in the optic chiasm: uncrossed axons diverge from crossed axons within a midline glial specialization. J Neurosci. 1995; 15:3716–3729. [PubMed: 7751940]

Messam CA, Hou J, Major EO. Coexpression of nestin in neural and glial cells in the developing human CNS defined by a human-specific anti-nestin antibody. Exp Neurol. 2000; 161:585–596. [PubMed: 10686078]

Mohler WA, Blau HM. Gene expression and cell fusion analyzed by lacZ complementation in mammalian cells. Proc Natl Acad Sci U S A. 1996; 93:12423–12427. [PubMed: 8901597]

Mori T, Wanaka A, Taguchi A, Matsumoto K, Tohyama M. Differential expressions of the eph family of receptor tyrosine kinase genes (sek, elk, eck) in the developing nervous system of the mouse. Brain Res Mol Brain Res. 1995; 29:325–335. [PubMed: 7609620]

Murai KK, Pasquale EB. 'Eph'ective signaling: forward, reverse and crosstalk. J Cell Sci. 2003; 116:2823–2832. [PubMed: 12808016]

Nagy A, Rossant J, Nagy R, Abramow-Newerly W, Roder JC. Derivation of completely cell culture-derived mice from early-passage embryonic stem cells. Proc Natl Acad Sci U S A. 1993; 90:8424–8428. [PubMed: 8378314]

Nakagawa S, Brennan C, Johnson KG, Shewan D, Harris WA, Holt CE. Ephrin-B regulates the Ipsilateral routing of retinal axons at the optic chiasm. Neuron. 2000; 25:599–610. [PubMed: 10774728]

Noren NK, Pasquale EB. Eph receptor-ephrin bidirectional signals that target Ras and Rho proteins. Cell Signal. 2004; 16:655–666. [PubMed: 15093606]

Orioli D, Henkemeyer M, Lemke G, Klein R, Pawson T. Sek4 and Nuk receptors cooperate in guidance of commissural axons and in palate formation. Embo J. 1996; 15:6035–6049. [PubMed: 8947026]

Petros TJ, Bryson JB, Mason C. Ephrin-B2 elicits differential growth cone collapse and axon retraction in retinal ganglion cells from distinct retinal regions. Dev Neurobiol. 2010; 70:781–794. [PubMed: 20629048]

Petros TJ, Shrestha BR, Mason C. Specificity and sufficiency of EphB1 in driving the ipsilateral retinal projection. J Neurosci. 2009; 29:3463–3474. [PubMed: 19295152]

Porter S, Larue L, Mintz B. Mosaicism of tyrosinase-locus transcription and chromatin structure in dark vs. light melanocyte clones of homozygous chinchilla-mottled mice. Dev Genet. 1991; 12:393–402. [PubMed: 1822431]

Rachel RA, Dolen G, Hayes NL, Lu A, Erskine L, Nowakowski RS, Mason CA. Spatiotemporal features of early neuronogenesis differ in wild-type and albino mouse retina. J Neurosci. 2002; 22:4249–4263. [PubMed: 12040030]

Rebsam A, Petros TJ, Mason CA. Switching retinogeniculate axon laterality leads to normal targeting but abnormal eye-specific segregation that is activity dependent. J Neurosci. 2009; 29:14855–14863. [PubMed: 19940181]

Shi Y, Pontrello CG, DeFea KA, Reichardt LF, Ethell IM. Focal adhesion kinase acts downstream of EphB receptors to maintain mature dendritic spines by regulating cofilin activity. J Neurosci. 2009; 29:8129–8142. [PubMed: 19553453]

Sretavan DW. Specific routing of retinal ganglion cell axons at the mammalian optic chiasm during embryonic development. J Neurosci. 1990; 10:1995–2007. [PubMed: 2162389]

Steingrimsson E, Copeland NG, Jenkins NA. Mouse coat color mutations: from fancy mice to functional genomics. Dev Dyn. 2006; 235:2401–2411. [PubMed: 16691561]

Thakar S, Chenaux G, Henkemeyer M. (Submitted).

Tronche F, Kellendonk C, Kretz O, Gass P, Anlag K, Orban PC, Bock R, Klein R, Schutz G. Disruption of the glucocorticoid receptor gene in the nervous system results in reduced anxiety. Nat Genet. 1999; 23:99–103. [PubMed: 10471508]

Webster MJ, Rowe MH. Disruption of developmental timing in the albino rat retina. J Comp Neurol. 1991; 307:460–474. [PubMed: 1856331]

Williams SE, Mann F, Erskine L, Sakurai T, Wei S, Rossi DJ, Gale NW, Holt CE, Mason CA, Henkemeyer M. Ephrin-B2 and EphB1 mediate retinal axon divergence at the optic chiasm. Neuron. 2003; 39:919–935. [PubMed: 12971893]

Wybenga-Groot LE, Baskin B, Ong SH, Tong J, Pawson T, Sicheri F. Structural basis for autoinhibition of the Ephb2 receptor tyrosine kinase by the unphosphorylated juxtamembrane region. Cell. 2001; 106:745–757. [PubMed: 11572780]

Xu NJ, Henkemeyer M. Ephrin-B3 reverse signaling through Grb4 and cytoskeletal regulators mediates axon pruning. Nat Neurosci. 2009; 12:268–276. [PubMed: 19182796]

Yokoyama N, Romero MI, Cowan CA, Galvan P, Helmbacher F, Charnay P, Parada LF, Henkemeyer M. Forward signaling mediated by ephrin-B3 prevents contralateral corticospinal axons from recrossing the spinal cord midline. Neuron. 2001; 29:85–97. [PubMed: 11182083]

Zhuo L, Theis M, Alvarez-Maya I, Brenner M, Willecke K, Messing A. hGFAP-cre transgenic mice for manipulation of glial and neuronal function in vivo. Genesis. 2001; 31:85–94. [PubMed: 11668683]
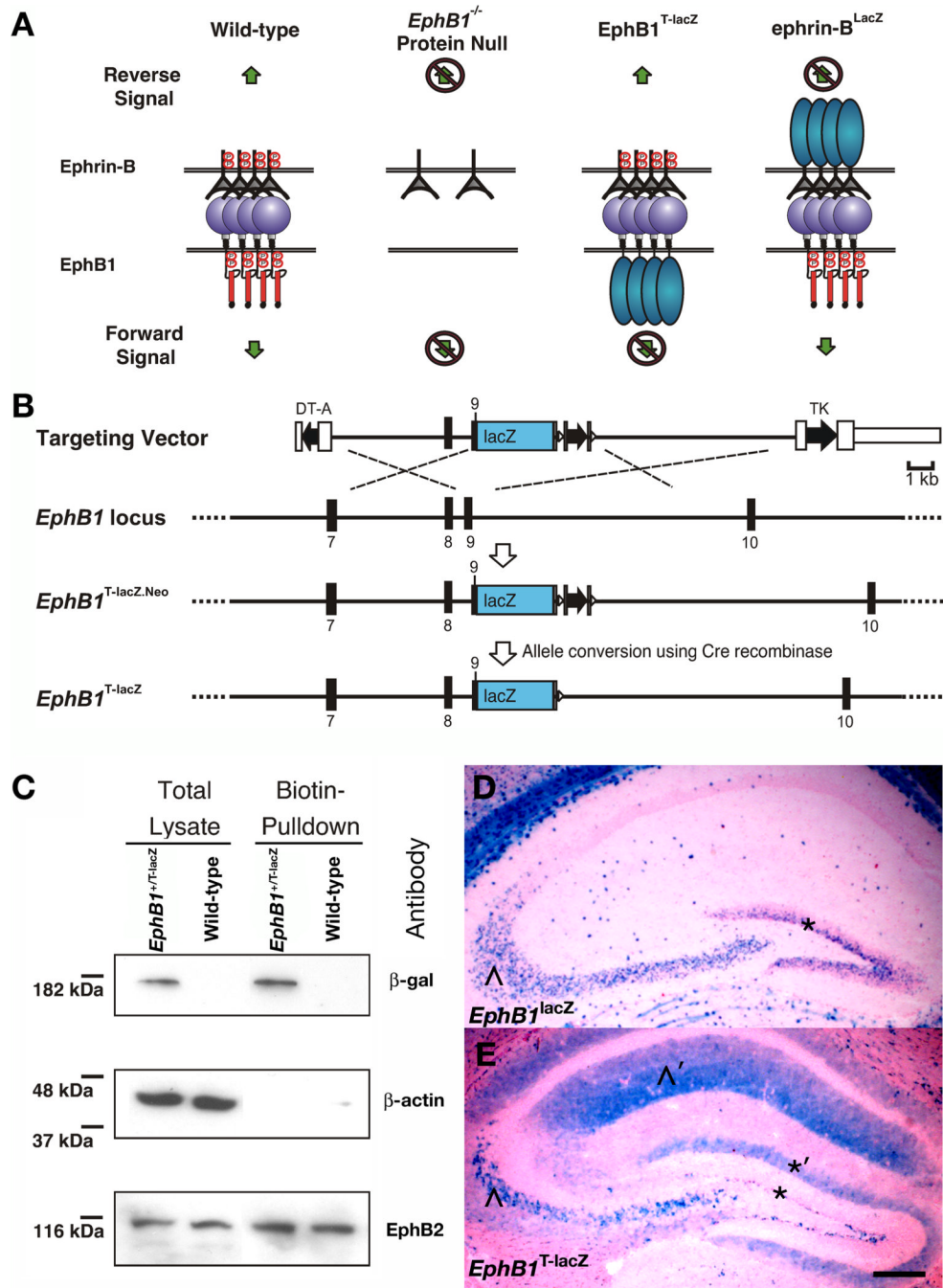
Fig. 1.
Generation and verification of truncated $EphB1^{T-lacZ}$ mutant mice. (A) A cartoon depicting EphB:ephrin-B bidirectional signaling and the consequence of $EphB1^-$ protein null, $EphB1^{T-lacZ}$ truncated (EphB1-β-gal fusion protein), and *ephrin-B*^{lacZ} truncated (ephrin-B-β-gal fusion protein) mutations. The protein null loses both forward and reverse signals, the EphB1-β-gal fusion is still able to stimulate reverse signals, and the ephrin-B-β-gal fusion is still able to stimulate forward signals. (B) Targeting strategy used to insert the *lacZ* open reading frame into the *EphB1* reading frame within exon 9 immediately following the codons for the transmembrane domain. The targeting vector contained two negative selection cassettes encoding diphtheria toxin-α (DT-A) and thymidine kinase (TK) on the 5'

and 3' end, respectively. (C) Immunoblot of proteins isolated from primary cells whose extracellular proteins were labeled with biotin and purified with streptavidin-agarose beads. Total protein lysates (left) of cells from wild-type and *EphB1*$^{+/lacZ}$ heterozygote littermate embryos collected at E13.5 were compared to the purified biotin-labeled fraction (right) using antibodies raised against β-gal for EphB1-β-gal fusion protein, β-actin as intracellular control, and EphB2 as extracellular control. (D) X-gal stains of hippocampal sections of adult *EphB1*^{lacZ} mice in D where β-gal activity is localized only in the cell bodies of CA3 neurons (^) and neural progenitors of the dentate gyrus (*) and *EphB1*$^{T-lacZ}$ mice in D' where staining is visible in both the cell bodies and their processes, including CA3 axons that target into the CA1 region (^') and in the extensions of subgranular zone progenitor cells that reach into the molecular layer of the dentate gyrus (*'). Scale bar = 200 µm.
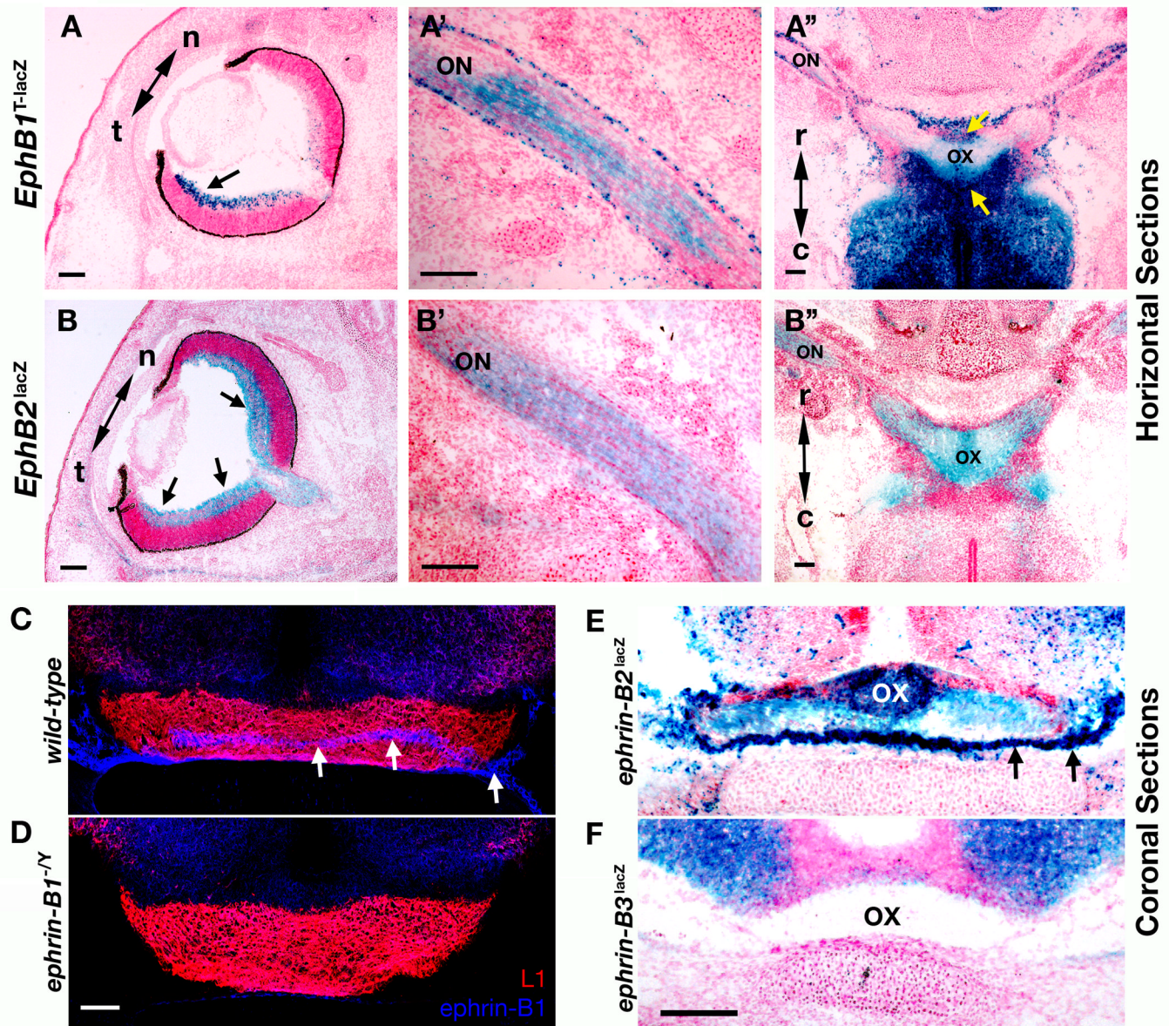
Fig. 2.

EphB and ephrin-B expression patterns at E16.5. (A and B) X-gal stains of horizontal sections at E16.5 show expression patterns of EphB1 and EphB2 β-gal fusion proteins (black arrows). An $EphB1^{\text{T-lacZ}}$ mouse eye (A) shows higher β-gal activity confined temporally (t) while (B) $EphB2^{\text{lacZ}}$ mice present β-gal activity from temporal to nasal (n) portions of the retina. Horizontal sections show that both EphB1 (A') and EphB2 (B') β-gal fusion proteins are transported down the optic nerve (ON). Horizontal sections through the optic chiasm (OX) show that both EphB1 (A") and EphB2 (B") β-gal fusion proteins are present at the optic chiasm originating from the ON, while EphB1 is uniquely present in the area surrounding the OX (yellow arrows). Scale bars = 100 µm. (C and D) Coronal section of an E16.5 wild-type mouse brain (C) with antibodies against L1 (red) to label the OX and ephrin-B1 (blue) to mark specific expression within and around the OX (white arrows) compared to the non-specific staining visible in an $ephrin\text{-}B1^{-/Y}$ mutant mouse (D) as a negative control. Scale bar = 50µm. (E and F) X-gal stains of coronal sections at E16.5 show

expression patterns within and surrounding the OX of ephrin-B2 (E, green arrows) and ephrin-B3 (F) β-gal fusion proteins. Scale bar = 100µm.
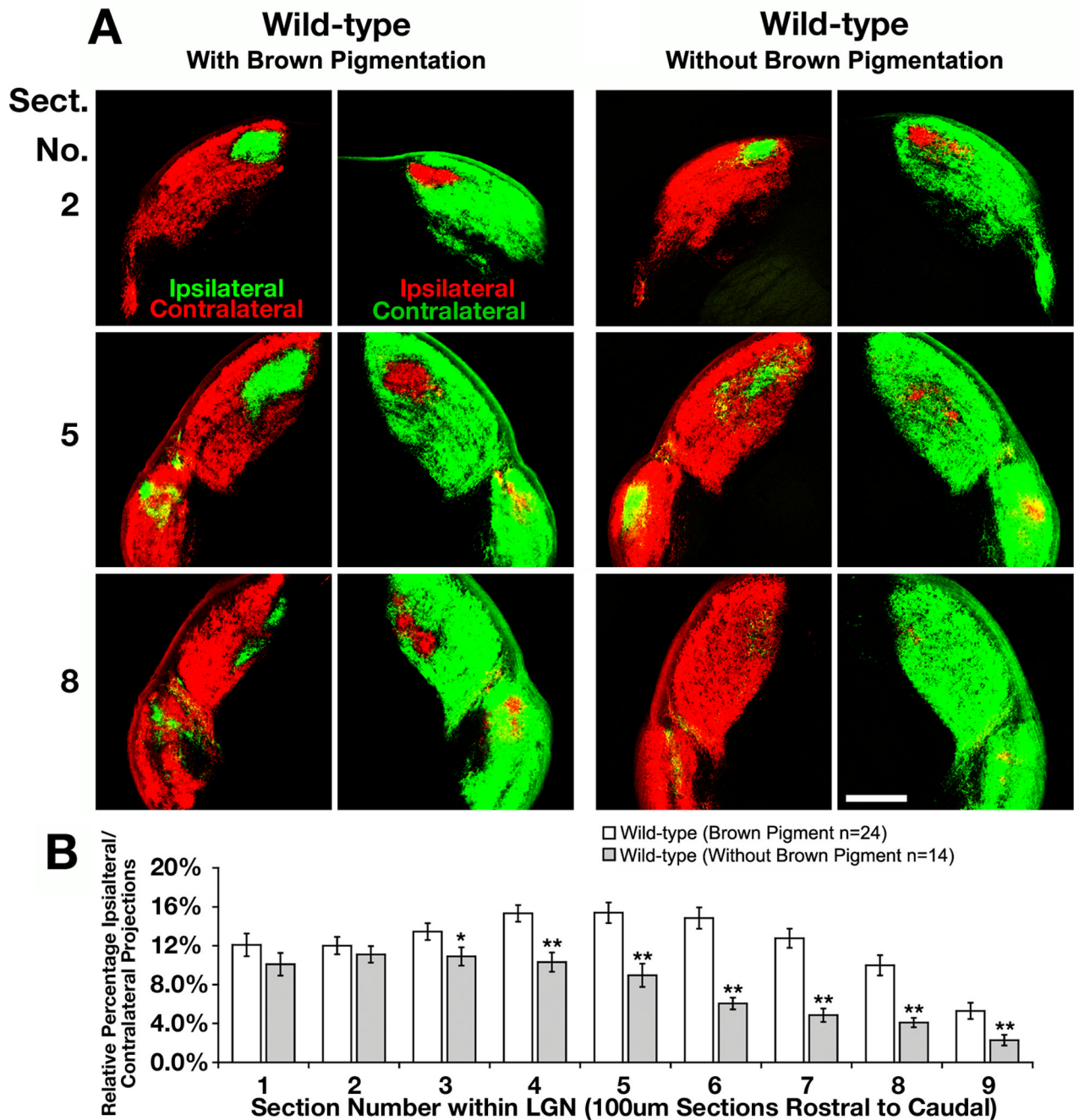
Fig. 3.
Brown pigmented mice possess a larger percentage of ipsilateral projections to the lateral geniculate nucleus than mice lacking brown pigmentation. (A) Serial sections through the lateral geniculate nucleus of a wild-type mouse with brown pigmentation and another without brown pigmentation. The retinal ganglion cells were labeled with cholera toxin subunit-B-555 (CTB-555, red) anterograde dye in right eye and CTB-488 (green) in the left eye to compare changes in the amount of ipsilaterally projecting RGC axons. Scale bar = 250 µm. (B) Quantitative analysis showing the differences in relative percentage of ipsilaterally projecting RGC axons throughout the entire lateral geniculate nucleus (LGN) of each genotype (* indicates $p<0.05$, ** indicates $p<0.01$).
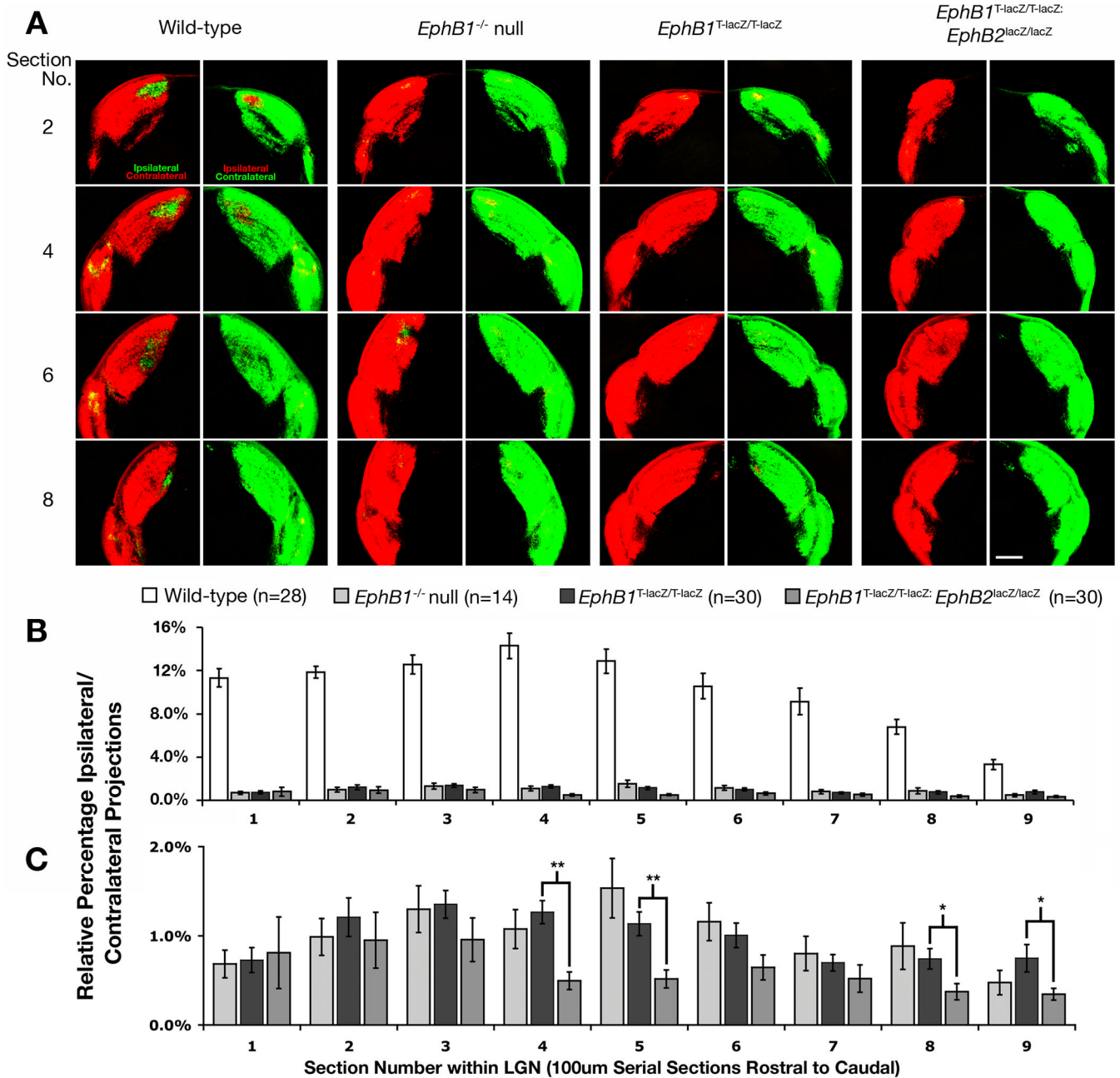
Fig. 4.

$EphB1^{\text{T-lacZ/T-lacZ}}$ mutant mice show a drastic decrease in the ipsilateral projection. (A) Representative regions of serial coronal sections through the LGN of wild-type, $EphB1^{-/-}$ null homozygote, truncated $EphB1^{\text{T-lacZ/T-lacZ}}$ homozygote, and $EphB1^{\text{T-lacZ/T-lacZ}}$: $EphB2^{\text{lacZ/lacZ}}$ compound homozygote mice. All RGCs were labeled with CTB-555 (red) in right eye and CTB-488 (green) in the left eye and allowed to anterogradely label their terminations in the LGN to compare changes in the amount of ipsilaterally projecting RGC axons. Scale bar = 250 µm. (B) Quantitative analysis showing the differences in relative percentage of ipsilaterally projecting RGC axons throughout the entire lateral geniculate nucleus of each genotype with wild-type. (C) A close-up of the above chart to highlight

differences in mutant phenotypes. (All mice are 90%CD1 strain; * indicates $p < 0.05$, ** indicates $p < 0.01$).
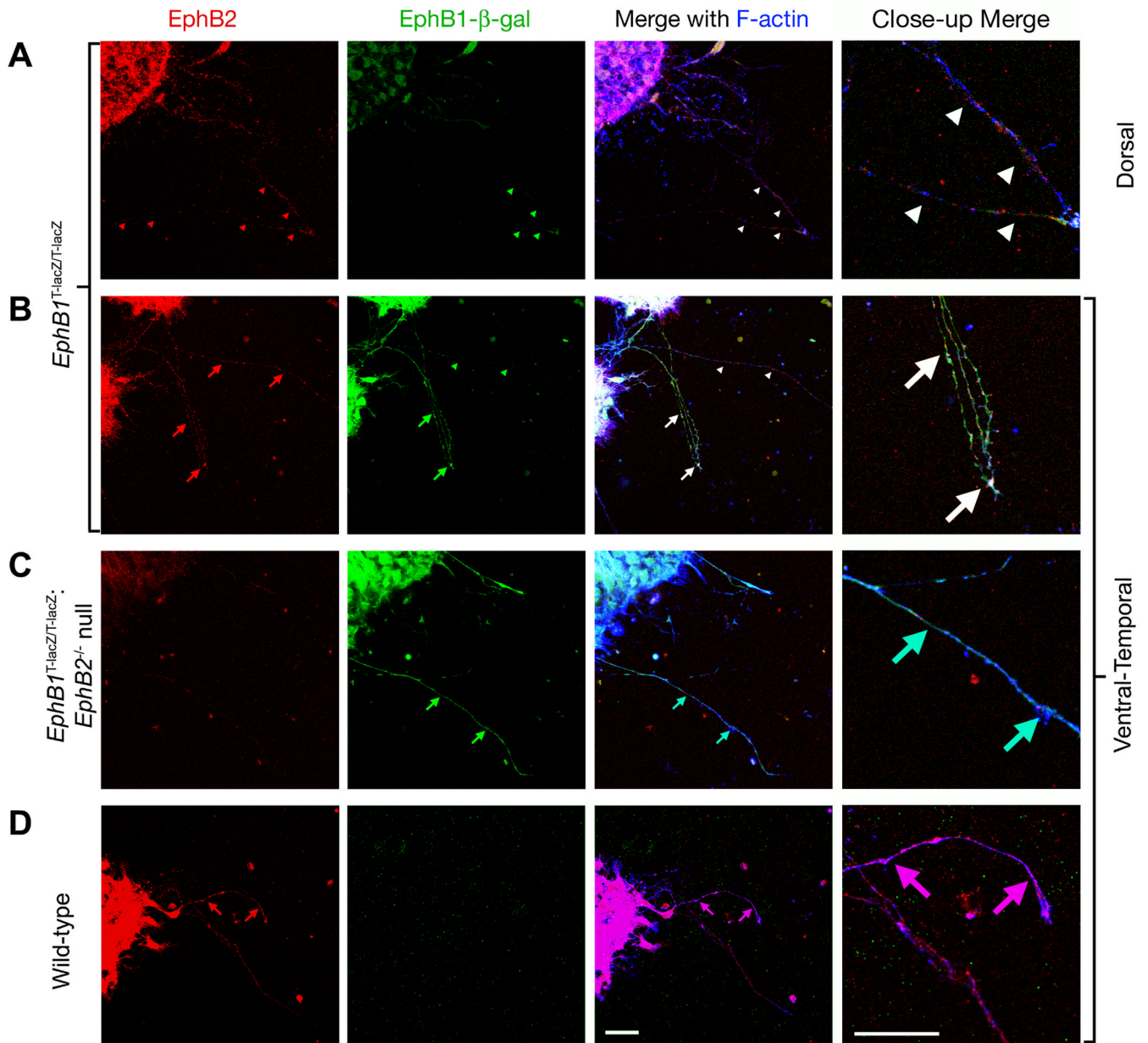
Fig. 5.
EphB1 and EphB2 are coexpressed in ventrotemporal RGC axons. Retinal explants from $EphB1^{\text{T-lacZ/T-lacZ}}$ (A and B), $EphB1^{\text{T-lacZ/T-lacZ}}$: $EphB2^{\text{lacZ/lacZ}}$ (C), and wild-type (D) E15.5 stage embryos were removed, cultured, exposed to a fluorescent substrate recognized by β-gal (green), immunostained with α-EphB2 antibodies (red), and exposed to phalloidin conjugated to cy-5 (blue). In A, retinal ganglion cells (RGCs) from the dorsal portion of the retina extended axons that co-express (white arrowheads) low levels of EphB2 (red arrowheads) and EphB1-β-gal (green arrowheads). In B, RGCs from the ventrotemporal portion of the retina extended axons with higher levels of EphB2 (red arrows), but only a subset of these coexpress high levels of EphB1-β-gal (green/white arrows). In C, $EphB1^{\text{T-lacZ/T-lacZ}}$: $EphB2^{-/-}$ mutant RGC axons from the ventrotemporal portion of the retina project axons with little to no visible EphB2 staining but high levels of β-gal activity.

In D, wild-type RGC axons from the ventrotemporal portion of the retina project axons with high levels of EphB2 and no visible β -gal activity. Scale bar = 20 µm.
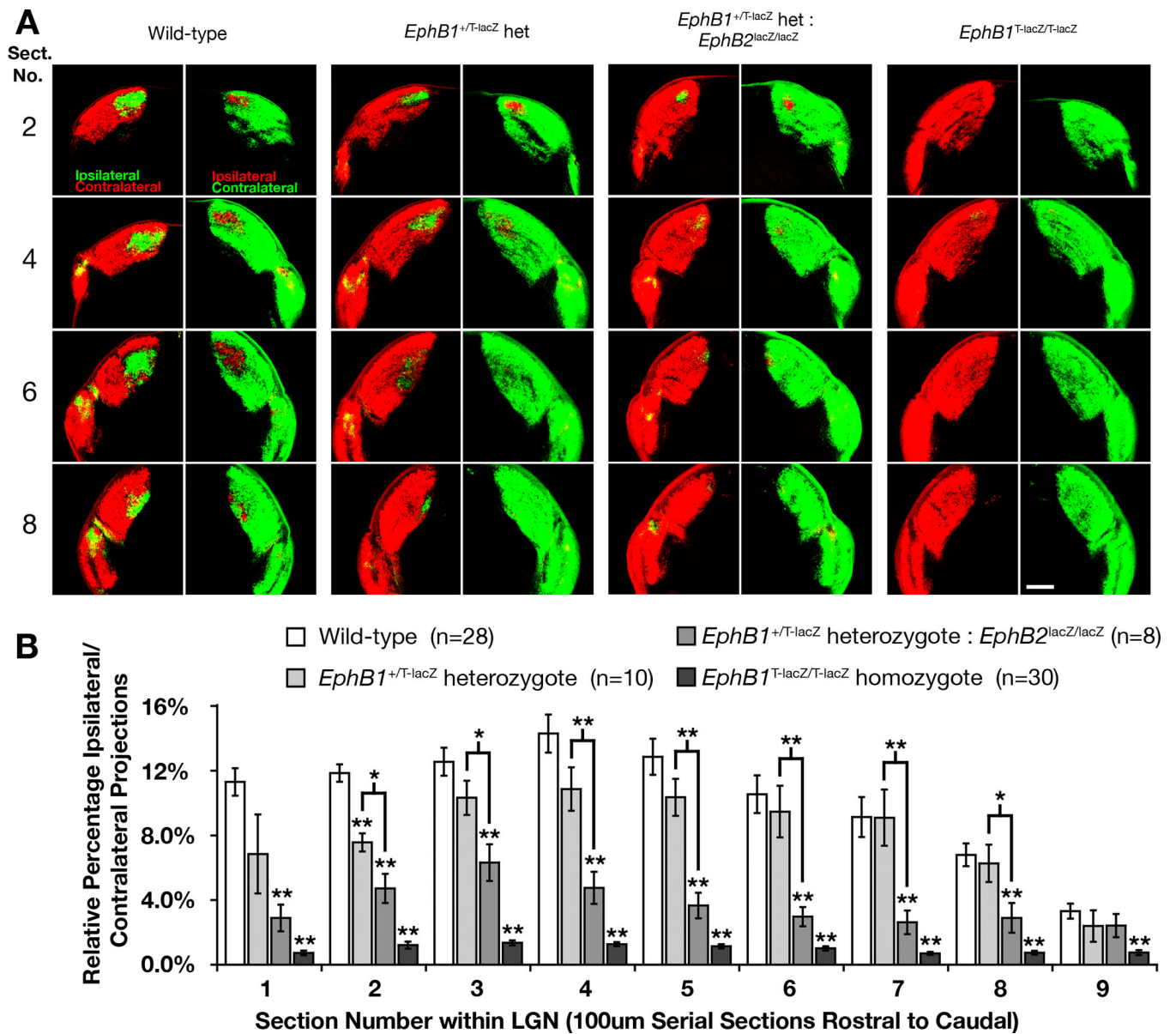
Fig. 6.
Reduced ipsilateral projections in mice with diminished EphB1 and EphB2 forward signaling. (A) Serial coronal sections through representative regions the lateral geniculate nucleus of wild-type, $EphB1^{+/T-lacZ}$ heterozygous, $EphB1^{+/T-lacZ}$ heterozygote: $EphB2^{lacZ/lacZ}$, and EphB1$^{T-lacZ/T-lacZ}$ homozygous mice. All RGCs were labeled with CTB-555 (red) in the right eye and CTB-488 (green) in the left eye to compare changes in the amount of ipsilaterally projecting RGC axons. Scale bar = 250 µm. (B) Quantitative analysis showing the differences in relative percentage of ipsilaterally projecting RGC axons throughout the entire lateral geniculate nucleus of each genotype (All mice are 90%CD1 strain; * indicates $p<0.05$, ** indicates $p<0.01$).
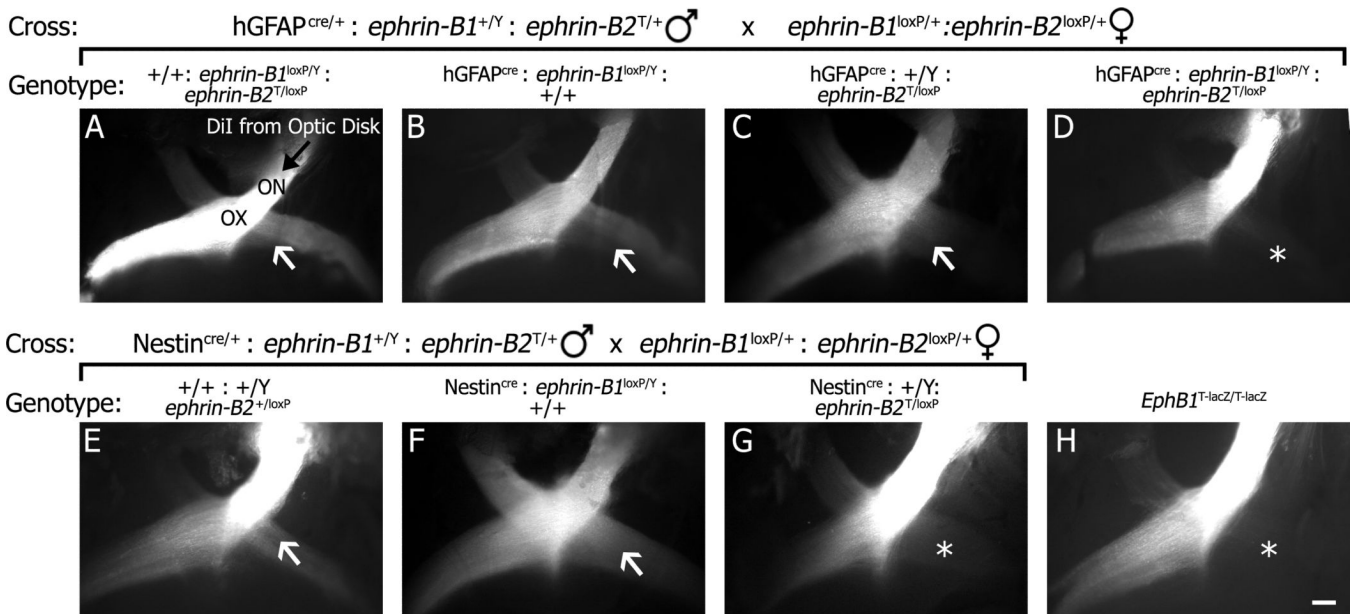
Fig. 7.
Conditional *ephrin-B* mutant mice display reduced ipsilateral projections at the optic chiasm. Direct visualization of optic chiasm of P0 mice where one optic nerve (ON) was labeled with DiI diffused from the optic disk (black arrow) to check for the presence (white arrow) or lack (*) of an ipsilateral projection from the optic chiasm (OX). (A–G) Two crosses (shown directly above images) were used to generate specific mutant mice of the following genotypes: *ephrin-B1*$^{loxP/Y}$: *ephrin-B2*$^{T/loxP}$ double mutant mice lacking cre recombinase under the hGFAP promoter (A), hGFAP^{cre}:*ephrin-B1*$^{loxP/Y}$ (B), hGFAP^{cre}:*ephrin-B2*$^{T/loxP}$ (C), hGFAP^{cre}:*ephrin-B1*$^{loxP/Y}$:*ephrin-B2*$^{T/loxP}$ (D), *ephrin-B2*$^{+/loxP}$ heterozygote mutant mice lacking cre recombinase under the Nestin promoter (E) Nestin^{cre}:ephrin-*B1*$^{loxP/Y}$ (F), and Nestin^{cre}:*ephrin-B2*$^{T/loxP}$ (G). (H) An *EphB1*$^{T-lacZ/T-lacZ}$ mutant mouse. The *ephrin-B2*^{T} mutation produces a truncated form of ephrin-B2 that fails to reach the cell surface and acts as a protein-null (Cowan et al., 2004). Scale bar = 200 µm.
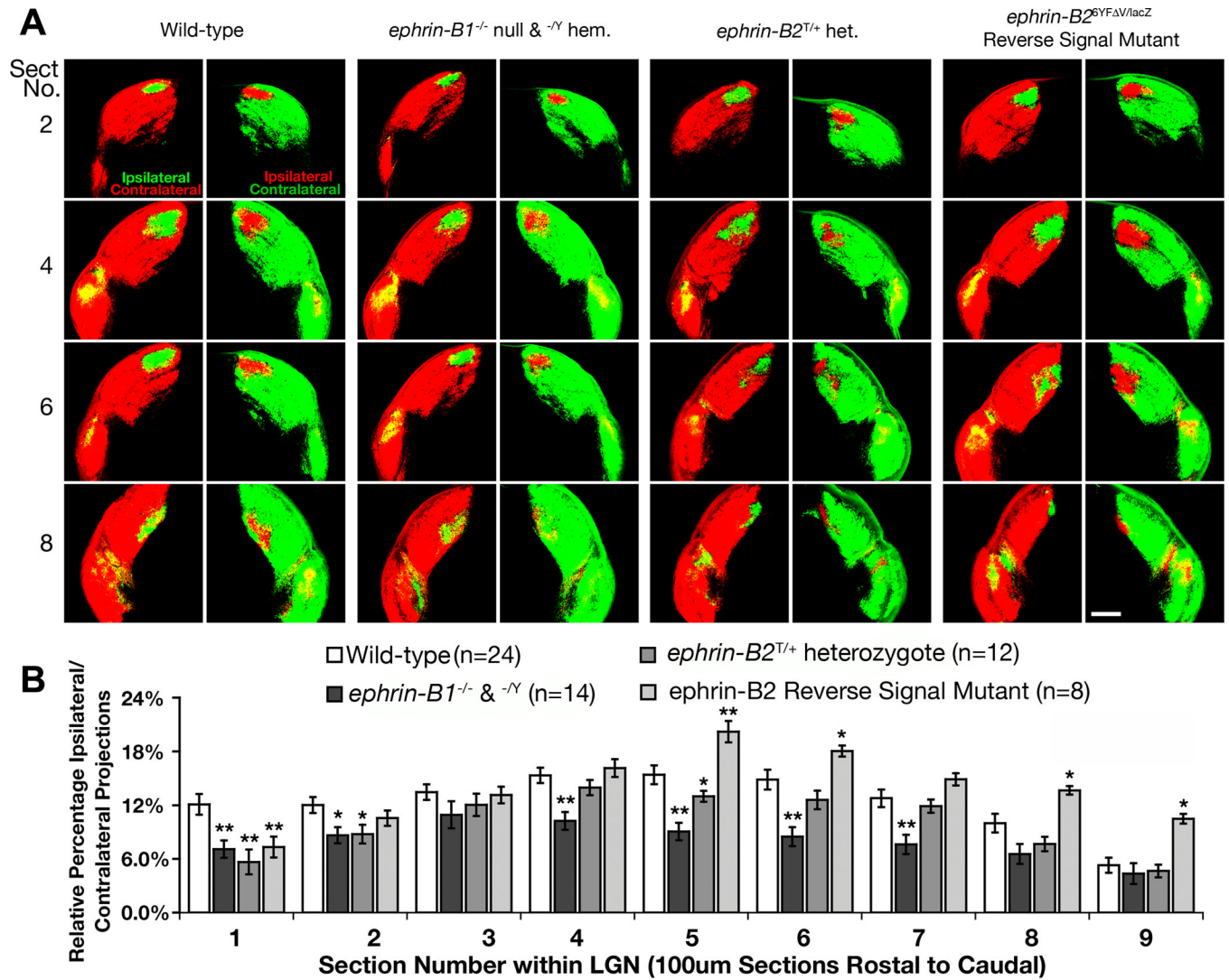
Fig. 8.
Ephrin-B1 and *ephrin-B2* mutant mice display reduced ipsilateral projections. (A) Serial sections through the lateral geniculate nucleus of wild-type, *ephrin-B1*$^{-/-}$ null and *ephrin-B1*$^{-/Y}$ hemizygous, *ephrin-B2*$^{+/T}$ heterozygote, and ephrin-B2$^{6YF\Delta V/lacZ}$ reverse signaling mice whose RGC axons were labeled with CTB-555 (red) in the right eye and CTB-488 (green) in the left eye to compare changes in the amount of ipsilaterally projecting RGCs. Scale bar = 250 µm. (B) Quantitative analysis showing the differences in relative percentage of ipsilaterally projecting RGC axons throughout the entire lateral geniculate nucleus of each genotype (All mice are 90%CD1 strain; * indicates p<0.05, ** indicates p<0.01).